Misorientation dependence of epitaxial growth on vicinal GaAs(001)

T. Shitara, D. D. Vvedensky, and M. R. Wilby*
The Blackett Laboratory, Imperial College, London SW7 2BZ, United Kingdom
and Interdisciplinary Research Centre for Semiconductor Materials, Imperial College, London SW7 2BZ, United Kingdom

J. Zhang, J. H. Neave, and B. A. Joyce
Interdisciplinary Research Centre for Semiconductor Materials, Imperial College, London SW7 2BZ, United Kingdom
(Received 27 January 1992)

The misorientation direction dependence of the transition from growth by the formation and coalescence of two-dimensional clusters to growth by step advancement has been examined systematically with reflection high-energy electron-diffraction (RHEED) measurements during molecular-beam epitaxy on GaAs(001). Accompanying simulations of a solid-on-solid model have reproduced qualitatively all of the dominant features of the measured RHEED through comparisons based upon the step densities of the simulated surfaces. We have reported earlier that the Ga flux and misorientation-angle dependence of RHEED on vicinal GaAs(001) surfaces misoriented towards the [010] direction can be both qualitatively and quantitatively reproduced by a suitably parametrized solid-on-solid model. Here, we have modified the model to account for the anisotropy in the surface kinetics expected for surfaces misoriented along the [110] and [$\bar{1}$10] directions. Two distinct origins of this anisotropy have been considered, both separately and together: one that is based only on the nearest-neighbor environment and one that is based on attempt frequencies for migration, which is independent of the nearest-neighbor environment. Both effects can contribute to the anisotropy of the diffusion constant and to the temperature at which growth becomes dominated by step advancement, but the growth-front morphologies differ considerably in the two cases. Although diffraction effects have impeded direct quantitative comparisons between measured RHEED and simulated step density on these surfaces, qualitative conclusions can still be made and simulated morphologies can be compared with scanning tunneling microscopy. Our comparisons suggest that the origin of the anisotropic growth-mode transition stems mainly from anisotropic incorporation kinetics, modeled by the nearest-neighbor environment, rather than anisotropic adatom mobility. Moreover, even if the mobility is anisotropic, the favored direction is orthogonal to that reported by others.

I. INTRODUCTION

Investigations of the growth on vicinal surfaces of III-V compound semiconductors by molecular-beam epitaxy (MBE) have shown that at sufficiently high temperatures growth occurs primarily by step advancement, with only slight remnants of two-dimensional clusters on the terraces.[1] This suggests the possibility of growing quantum wires directly without the use of lithography[2] and, in principle, reduces interface roughness.[3] It has, in fact, been reported that quantum wires grown by MBE on vicinal GaAs(001) surfaces misoriented toward the [110] direction (subsequently denoted as the "*A*" surface) have shown strong periodic modulations in transmission electron microscopy and diffraction, while those grown on (001) surfaces misoriented towards [$\bar{1}$10] (the "*B*" surface) have not.[4]

Virtually all III-V semiconductors have the zinc-blende structure, which means that the step structure will depend on the direction of misorientation of the vicinal surface. Scanning tunneling microscope (STM) images have shown that there are appreciable differences between steps on *A* and *B* surfaces.[5] On the former, the step edge is smooth in the sense that there are relatively few kink sites, but on the latter the step edge is very rough. Several studies[6–8] of the temperature dependence of reflection high-energy electron-diffraction (RHEED) intensity oscillations on vicinal GaAs(001) substrates have shown that the transition temperature (T_c) between two-dimensional nucleation and step advancement depends on the misorientation direction. In general, for the same growth conditions (fluxes, angle of misorientation, etc.), T_c is higher on *A* surfaces than *B* surfaces, with that for the "*C*" surface (misoriented toward the [010] direction) occurring between them.

There are two surface kinetic processes that can exhibit anisotropy: the migration of adatoms (cations) on the terraces and the incorporation at the step edge through attachment and detachment rates. From RHEED measurements Ohta, Kojima, and Nakagawa[6] concluded that the surface diffusion constant was four times greater in the [$\bar{1}$10] direction than the [110]. Kawabe and Sugaya[9] observed that the growth rate was much larger in the [$\bar{1}$10] than the orthogonal [110] direction, which they also attributed to anisotropic diffusion. These conclusions were based on the assumptions that step structures were identical and step edges were perfect sinks, although other authors[7,8] have suggested that anisotropic step structures could influence the results. If steps act as perfect sinks for adatoms (no detachment occurs), faster

migration rates will lead to higher incorporation rates, although this may not be the case if detachment does occur, particularly if the anisotropy in the detachment rates acts *in competition* to the anisotropy in the mobility. It is, however, impossible to identify the origin of the anisotropy by measuring only T_c, since the growth-mode transition can be induced both by the surface migration of adatoms and also their incorporation at steps. The information that can be obtained from T_c is a convolution of both effects.

A potential solution of this problem is to compare RHEED intensity oscillations with Monte Carlo simulations of a growth model. This approach offers several benefits in attempting to identify the origins of the anisotropy resulting from different misorientations. First, the effect of each source of anisotropy can be introduced independently and to varying degrees to determine the role each has on the growth kinetics. Simulations are an ideal tool for investigating interacting processes that can act either in concert or in opposition. Second, based upon earlier comparisons between RHEED measurements and simulations,[10] a parametrization of the model that reproduces quantitatively the trends in T_c and even many features of the specular intensity evolution is an indication that the dominant kinetic processes have been included in the model. Thus, in making such comparisons, we are not limited to a narrow regime of substrate temperatures and fluxes near T_c, so we can investigate the *approach* to T_c as a function of growth conditions. Third, the effect of introducing refinements to the basic model through additional processes, e.g., bias in hopping up or down steps, can be easily addressed. Thus, the *stability* of the predictions of the model to perturbations can be addressed, i.e., is any agreement between simulations and measurements fortuitous?

In this paper we report the results of systematic RHEED measurements of the growth-mode transition and surface morphology on *A*, *B*, and *C* GaAs(001) surfaces. Accompanying simulations of a solid-on-solid model of MBE are also presented and used to analyze the measurements in the spirit of our earlier work.[10] Each of the two sources of anisotropy, adatom migration, and incorporation at steps, is first introduced separately to determine the individual effects of these processes upon the features of the growth. Although the anisotropy of each of these processes can cause changes in T_c, only an anisotropy in the incorporation rates reproduces the anisotropy in the step morphologies observed in STM measurements.[5] This fact, supported by direct comparisons with RHEED measurements, allows us to conclude that the dominant source of the anisotropy is due to the incorporation kinetics at step edges. We cannot rule out a contribution from the anisotropy in the adatom migration, but even if present, the favored direction is orthogonal to that suggested in Refs. 6 and 9.

The outline of this paper is as follows. The experimental methods are outlined in Sec. II and the experimental results presented in Sec. III. As in our study of growth on the *C* surface of GaAs(001), particular attention has been paid to the diffraction conditions used in making the RHEED measurements, and in maintaining the growth conditions as constant as possible. Both of these procedures have been made in order to satisfy as far as possible the basic assumptions of the solid-on-solid model. The model used for the simulations is described in Sec. IV. Several modifications of the model used in Ref. 10 have been introduced to characterize the anisotropy in the incorporation and adatom mobility. The physical motivation for our choices are discussed in Sec. IV. The analysis of the RHEED measurements using simulations of our model are carried out in Sec. V, including the determination of the model parameters and direct comparisons with the RHEED specular intensity oscillations. Section VI sets out our conclusions.

II. EXPERIMENTAL METHODS

All measurements were carried out in a purposely built MBE system described previously.[11] Etch-free n^+ GaAs(001) substrates (supplied by Sumitomo Electric) misoriented by $2\pm0.05°$ and $3\pm0.05°$ towards [110], $1\pm0.05°$, $2\pm0.05°$, and $3\pm0.05°$ toward [010], and $1\pm0.05°$ and $2\pm0.05°$ towards $[\bar{1}10]$ were used to avoid problems associated with wet etching. After *in situ* removal of the oxide film by heating to 630 °C under an incident As_2 flux a buffer layer at least 1000 Å thick was grown at 550 °C to provide a damage-free, reconstructed surface.

Ga fluxes were determined from the period of RHEED oscillations during growth at a substrate temperature of 560 °C and those of As_2 from arsenic-induced RHEED oscillations at approximately 530 °C,[12] in both cases on singular surfaces ($0\pm0.05°$), using the same beam azimuth as for the vicinal surfaces. The oscillation period in this system is very stable and there are no fluctuations associated with shutter operations. The measured As_2 flux (more correctly the incorporation rate) is, however, strongly dependent on substrate temperature and the quoted values are subject to this limitation.

The electron-beam energy was 14 keV with an incident (polar) angle of approximately 1°, as calculated from the angular separation between the straight-through and specular beams. This value was chosen to minimize complications from Kikuchi crossings on the 00 rod.[11,13] The specular beam intensity was measured with a photon-counting system and all shutter operations were computer controlled. The experiments were carried out for a growth and recovery sequence consisting of the deposition of four monolayers followed by a recovery period of equal duration. We began measurements at high temperatures and moved to lower temperatures to avoid any residual clusters formed by nucleation at the lower temperatures.

Since it is essential for the incident beam to be parallel to the step edges, the azimuth must be varied for the different directions of misorientation. This, however, has an effect on the phase of the oscillations.[14] For example, if we define the phase as the time to the first oscillation maximum normalized by the steady-state period on the singular surface, the values obtained at a substrate temperature of approximately 590° along the indicated directions are $[010]=1.00$, $[110]=0.90$, and $[\bar{1}10]=1.08$.

These ratios depend only weakly upon the temperature. Since the phase shift of the oscillations is related to the Kikuchi-like features[13] and because we are unable to evaluate the validity of the direct comparison with simulations until we can estimate the contribution from the Kikuchi-like features, we cannot carry out the same type of quantitative comparisons between RHEED measurements and simulations for the A and B surfaces as we did in Ref. 10 for the C surface. Even if we change the incident angle for each azimuth to avoid this phase shift, we have to separate the incident polar-angle-dependent contribution from the incident azimuthal dependence. Additionally, in the [$\bar{1}$10] azimuth, the surface reconstruction must have a strong interaction with the specular intensity because fractional-order rods exist close to the 00 rod. Therefore, the comparisons between simulations and experiments in Sec. V will be carried out only at a qualitative level.

III. EXPERIMENTAL RESULTS

The misorientation direction dependence of the growth-mode transition for surfaces misoriented by 2° is shown in Fig. 1, from which it is clear that $T_c(A) > T_c(C) > T_c(B)$, in agreement with previous work. The waveform of the oscillations also shows a misorientation direction dependence, e.g., the rate of damping is very fast on the B surface, where typically only one oscillation is discernible, even at the lowest temperatures. There is also an apparent anomaly with regard to the onset of oscillations on the A surface. At low temperatures there is an initial decrease of intensity, as expected, but which at higher temperatures changes to an initial intensity *increase*. This, however, is related to the surface reconstruction[11] because there is a fourfold reconstruction in the [$\bar{1}$10] azimuth and the effect disappears when the azimuth is changed to a few degrees away from an exact [$\bar{1}$10]. We have reported separately[14] that the oscillation period gradually increases as T_c is approached from below (measured as the delay to the first maximum with respect to that measured on a singular surface with identical growth conditions) and this behavior is apparent in

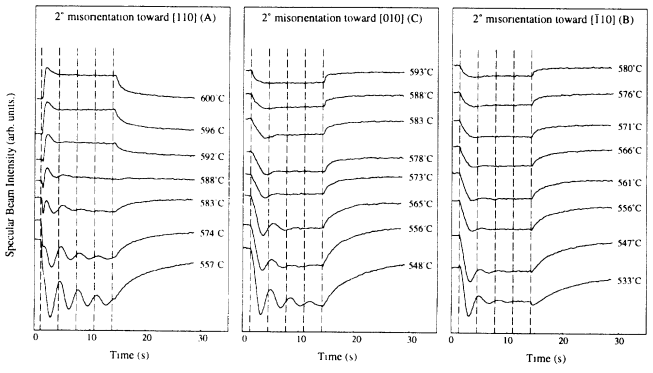

FIG. 1. The growth-mode transition on a vicinal GaAs(001) surface misoriented by 2° towards [110], [010], and [$\bar{1}$10]. The Ga flux is set at 0.31 ML/s and the As/Ga ratio is approximately 2.5. Monolayer deposition increments of Ga are indicated by dashed lines.

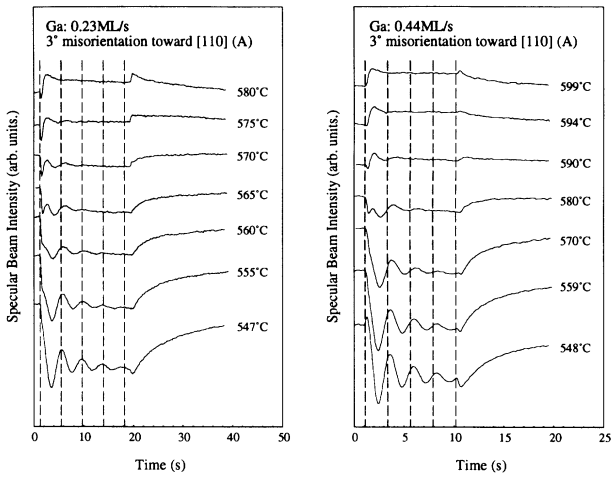

FIG. 2. The Ga flux dependence of the RHEED specular intensity near the transition from growth by nucleation of islands to growth by step advancement on an A surface misoriented by 3°.

all of the data reported here.

The effects of Ga flux and angle of misorientation are the same for all three directions of misorientation and the results are shown in Figs. 2–4. The Ga flux dependence of T_c on an A surface misoriented by 3° and a B surface misoriented by 1° are shown in Figs. 2 and 3, respectively, while Fig. 4 shows the Ga flux dependence for a misorientation of 2° in all three directions. In general, an increase in terrace length (smaller misorientation) increases T_c as does an increase in Ga flux, i.e., any increase in the encounter probability of Ga adatoms increases T_c.

The influence of the arsenic flux is, however, more complicated.[15] For a constant Ga flux, increasing the arsenic flux on B and C surfaces leads to a decrease of T_c, while on an A surface there is a corresponding increase. Results for A and B surfaces are shown in Fig. 5. The factors that can cause an increase in T_c all lead to an in-

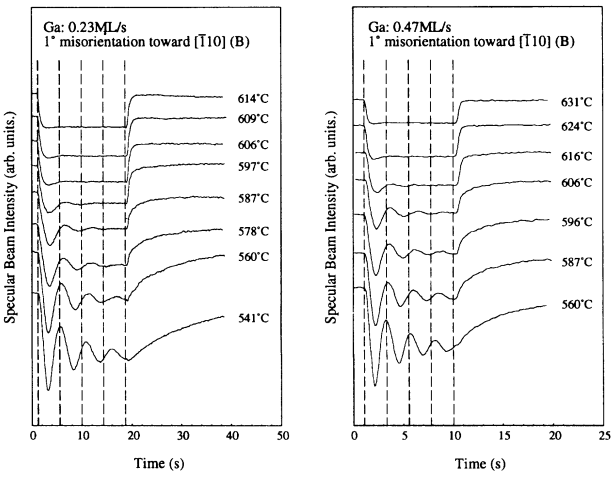

FIG. 3. The Ga flux dependence of the RHEED specular intensity near the transition from growth by nucleation of islands to growth by step advancement on B surface misoriented by 1°.

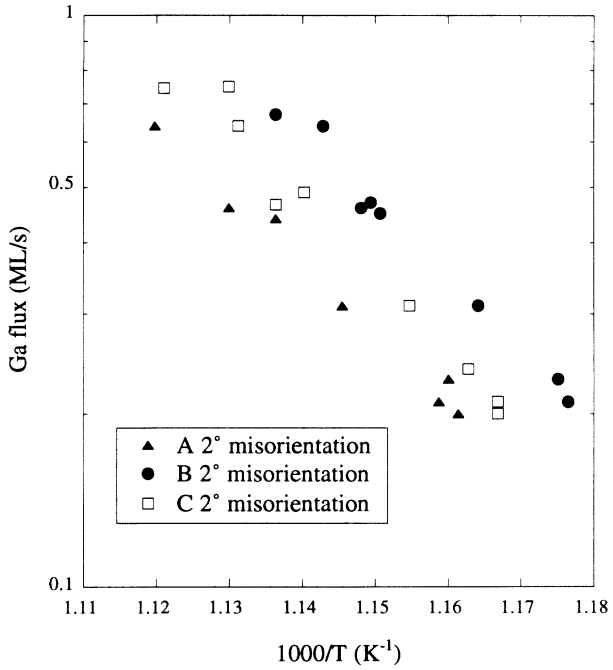

FIG. 4. Arrhenius plot showing the Ga flux and misorientation-direction dependence of the growth-mode transition temperature T_c on A, B, and C surfaces misoriented by 2°.

crease in the probability that migrating Ga adatoms interact on the terraces to form incipient clusters. This can be either a direct effect, such as an increase of the Ga flux or a decrease in the misorientation angle, as discussed above, or indirect, such as a decrease in the adatom mobility or an increase in the adatom concentration on the terraces due to an increase in the detachment rate from step edges. To reduce T_c, we have either to enhance Ga migration, inhibit island formation, or enhance Ga incorporation into the staircase steps. However, since the terraces on A and B surfaces are equivalent GaAs(001) surfaces away from the step edges, the island *formation* is the same on these surfaces. Therefore, the As flux must influence either Ga adatom migration, Ga incorporation at steps, or both of these processes. In fact, in our earlier work on the C surface,[10] a preliminary study of the effect of varying the As_2 flux was seen to be primarily a change in the incorporation rates, with only a comparatively

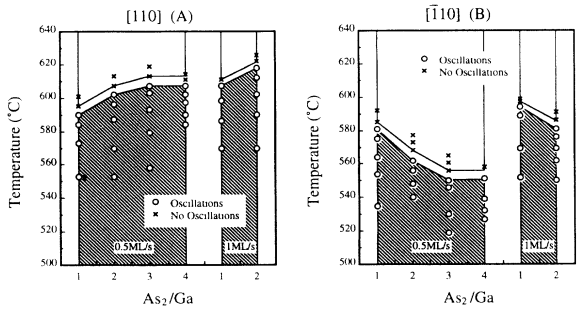

FIG. 5. The As flux and misorientation direction dependence of the growth-mode transition on A and B surfaces.

slight change in the adatom mobility. The comparisons with simulations reported below confirm these initial findings.

IV. GROWTH MODEL

We apply a model previously used in Monte Carlo simulation studies of growth kinetics on vicinal surfaces.[16] The substrate is modeled as a simple cubic lattice, in which neither vacancies nor overhangs are permitted.[17] The model focuses upon the cation kinetics, as under sufficiently arsenic-rich conditions the Ga-As_2 (or As_4) reaction kinetics are not rate-limiting steps[18] for the growth. Thus, the effect of the As reaction and migration kinetics are assumed to affect the growth only quantitatively, i.e., in a manner that can be absorbed into changes in the migration parameters. Similarly, the presence of any surface reconstruction is subsumed in effective migration parameters, i.e., no explicit account of the surface reconstruction is required if the reconstruction does not change. In the work reported here the 2×4 reconstruction was maintained for all growth conditions.

Two processes are included in the description of the growth: random deposition of atoms onto the substrate and surface migration. Growth is initiated by the random deposition of atoms onto the lattice at a rate Ja^2 per site, where J is the flux and a is the nearest-neighbor distance (so a^2 is the area per site). Surface migration rates are expressed by an Arrhenius expression for the nearest-neighbor hopping rate,

$$k(E,T)=k_0\exp(-E/k_BT)\ , \tag{1}$$

where k_0 is the vibrational frequency of a surface atom, T is the substrate temperature, E is the energy barrier to hopping, and k_B is Boltzmann's constant.

The parameters in the model are contained entirely within Eq. (1). For a model with lateral interactions and nearest-neighbor hopping both being isotropic, k_0 can be estimated by treating the vibrations of adatoms as classical harmonic oscillators and applying the equipartition to obtain $k_0=2k_BT/h$ for the vibrational frequency, where h is Planck's constant. The barrier is taken to be comprised of two terms, one due to the substrate alone, E_S, and a contribution E_N from each lateral nearest neighbor. This model was parametrized in Ref. 10 for the C surface with an As/Ga ratio of approximately 2.5, with the results

$$E_S=1.58\pm0.02\ \text{eV},\quad E_N/E_S\simeq0.15\ . \tag{2}$$

It must be stressed that the numerical values of E_S and E_N depend upon factors not explicitly included, most notably, the As/Ga ratio and the surface reconstruction.

To make even qualitative comparisons with RHEED measurements on A and B surfaces, this model must be modified to include the influence of the anisotropy on the migration and incorporation of adatoms. This anisotropy is due both to the crystal structure of GaAs (zinc-blende structure) and anisotropic 2×4 reconstruction on GaAs(001). We distinguish between two types of effects: one that originates in the nearest-neighbor environment

and one that is applied in the same way to all atoms and is independent of the nearest-neighbor environment. In the former case, we focus on the hopping barrier E in Eq. (1) and in the latter on the attempt frequency k_0. Even though our model does not include a 2×4 unit cell explicitly, the surface morphologies produced by our simulation can show at least the qualitative features of the anisotropy.

To introduce anisotropy into the lateral interactions, the hopping barrier is modified in the following manner:

$$E=E_S+mE_{[\bar{1}10]}+nE_{[110]}\ , \tag{3}$$

where m and n are the number of nearest neighbors in the $[\bar{1}10]$ and [110] directions, respectively, i.e., $m,n=0,1,2$, and $E_{[\bar{1}10]}$ and $E_{[110]}$ are the contributions to the diffusion barrier of each nearest neighbor along these directions. For GaAs(001), the anisotropy depends upon the misorientation directions, since there are two types of Ga—As—Ga bonds. Along the $[\bar{1}10]$ direction, Ga atoms have bonds with As atoms in lower layers, but along the [110] direction, with As atoms in upper layers. This suggests that $E_{[\bar{1}10]}$ is greater than $E_{[110]}$. When step edges are involved, on the A surface each Ga forms only three As bonds because one of the upper As atoms is free, while on the B surface each Ga makes four As bonds (Fig. 6). As-As dimerization on a 2×4 reconstructed surface may also make an additional energy contribution in the $[\bar{1}10]$ direction. In other words, it is more difficult to detach Ga atoms from As-terminated steps than from Ga-terminated steps. In the simulations reported below, we have therefore taken $E_{[\bar{1}10]}>E_{[110]}$, and have parametrized the migration barriers in terms of the average E_N and the ratio Δ_E of the two lateral barriers,

$$E_N=\tfrac{1}{2}\{E_{[\bar{1}10]}+E_{[110]}\},\quad \Delta_E=\frac{E_{[\bar{1}10]}}{E_{[110]}}\ . \tag{4}$$

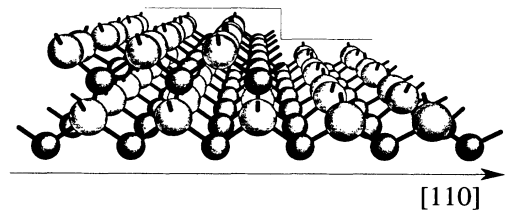

A surface (Ga terminated)

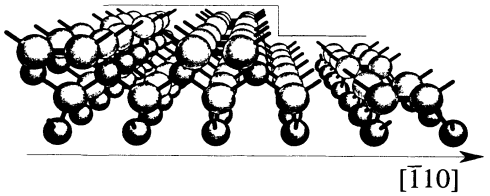

B surface (As terminated)

FIG. 6. Schematic illustration of the GaAs(001) 2×4 reconstruction and the different step structures.

Anisotropy in adatom migration can be attributed to either or both of the anisotropies in the frequency prefactor and the barriers to hopping. The difference between these lies primarily in the temperature dependence, with the prefactor providing a much weaker change with temperature than the effect of the barrier anisotropy. Based upon an Einstein model of diffusion, Ohta, Kojima, and Nakagawa[6] conclude that the anisotropy is confined to the prefactor, since the activation energies obtained where the same for the A and B surfaces. Although conclusions based upon measurements of T_c alone must be interpreted with great care, we will consider initially anisotropies in the attempt frequency only. We suppose that the vibrational frequencies $k_{[\bar{1}10]}$ and $k_{[110]}$, along the $[\bar{1}10]$ and [110] directions, are unequal. Thus, while in the case of isotropic adatom migration the direction of hopping is chosen randomly and with equal probability for all nearest-neighbor sites, for anisotropic vibrational frequencies, the direction of the chosen site is weighted in favor of the direction with the greater frequency.

Since the transition temperature on the A surface is higher than that on the B surface, the adatom must migrate along the $[\bar{1}10]$ direction faster than the [110] direction if the step edges act as isotropic sinks. A possible origin of anisotropic hopping of single adatoms is surface reconstruction (Fig. 6), but the favored hopping direction must depend on the state of Ga adatoms. If Ga adatoms are physisorbed on the surface, the $[\bar{1}10]$ direction is favored. Since the As dimer bonds are along $[\bar{1}10]$, Ga atoms rarely encounter the As dimer bonds because there are channels in that direction, especially at the missing As-As dimers on a 2×4 reconstructed surface.[19] If the Ga adatoms are chemisorbed it is more difficult to break up As-As dimers in the $[\bar{1}10]$ direction than to hop to neighboring sites along the [110] direction. This is to be compared with the case of Si(001) 2×1, where it is likely that the surface diffusion is faster along the dimers in the underlying layer.[20,21] In analogy with our parametrization in (4), we introduce the average vibrational frequency k_0 and the ratio Δ_k,

$$k_0=\tfrac{1}{2}\{k_{[\bar{1}10]}+k_{[110]}\},\quad \Delta_k=\frac{k_{[\bar{1}10]}}{k_{[110]}}\ . \tag{5}$$

The measurements reported by Ohta, Kojima, and Nakagawa[6] suggest that $\Delta_k=4$.

The simulations are monitored by following the evolution of the step density, $S(\phi)$, projected along a given direction specified by the azimuthal angle ϕ ($\phi=0$ in the [110] direction):

$$S(\phi)=L^{-1}\sum_{i,j}\{[1-\delta(h_{i,j},h_{i+1,j})]\cos\phi + [1-\delta(h_{i,j},h_{i,j+1})]\sin\phi\}\ , \tag{6}$$

where $\delta(i,j)$ is the Kronecker delta, $h_{i,j}$ is the height of the column of atoms at the lattice site (i,j), and L is the number of sites on the lattice. Since the incident RHEED beam is directed perpendicular to the misorientation direction, we have monitored $S(\frac{1}{2}\pi)$ for the A surface, $S(0)$ for the B surface, and $S(\frac{1}{4}\pi)$ for the C surface.

In our previous work, we demonstrated that with a

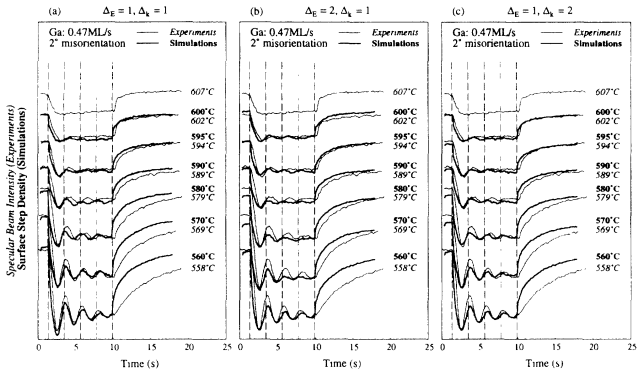

FIG. 7. Direct comparison between the measured RHEED oscillations and the simulated surface step density evolutions on the C surface. (a) $\Delta_E = 1$ and $\Delta_k = 1$, (b) $\Delta_E = 2$ and $\Delta_k = 1$, and (c) $\Delta_E = 1$ and $\Delta_k = 2$.

judicious choice of diffraction conditions the step density provides an excellent representation of the evolution of specular RHEED intensities for a variety of Ga fluxes and misorientation angles on the C surface.[10] Figure 7(a) shows a direct comparison between the measured RHEED oscillations and the simulated step density for an isotropic model on a C surface. The comparison for a given Ga flux and misorientation was made by rescaling the step density by the *same factor* for different temperatures. Specific quantitative features that are reproduced by the step density are approximately the same relative change of amplitude as function of temperature, including the initial decrease in the intensity at the start of growth as a function of temperature, the amplitude of the oscillations at low temperatures, and the steady-state intensities at high temperatures. In addition, there are several important qualitative similarities between the step density and the RHEED measurements, including the gradual disappearance of the oscillations with increasing temperature, the decaying envelope of the oscillations, the shapes of the oscillations, and the longer delay with increasing temperature of the first maximum of the oscillations.

V. COMPARISONS BETWEEN SIMULATIONS AND EXPERIMENTS

To determine which combination of the two possible processes produces the observed anisotropy, we first introduced them separately into the simulations. For $\Delta_E > 1$ [$\Delta_E = 2$ in Fig. 8(a)] and $\Delta_k = 1$, which corresponds to attachment anisotropy, T_c is higher on the A surface than the B, while the oscillations damp with time more rapidly on the latter. For $\Delta_k > 1$ [$\Delta_k = 2$ in Fig. 8(b)] and $\Delta_E = 1$, corresponding to migration anisotropy, T_c is again higher on the A surface and for both models the delay to the first oscillation maximum with increasing temperature is greater on the B than the A surface. All of the observed differences become more pronounced as Δ_E and Δ_k increase.

To a first approximation, the anisotropies on the C surface can be considered as being an average of those on A and B surfaces. This assertion was used in Ref. 10 to simplify the number of free parameters in the growth model. To provide some justification for this, we have compared measured oscillations and simulated step densities for $\Delta_E = 1$, $\Delta_k = 1$ [Fig. 7(a)], $\Delta_E = 2$, $\Delta_k = 1$ [Fig. 7(b)], and $\Delta_E = 1$, $\Delta_k = 2$ [Fig. 7(c)]. From the comparisons in Fig. 7 it is clear that the general similarities between the simulations and the measurements are not significantly different, although there might be a small improvement in the prediction of the increasing period as T_c is approached from below for both types of anisotropy.

The difference between the two possible origins of anisotropy becomes clear when the surface step densities projected onto the two orthogonal $\langle 110 \rangle$ directions on a C surface are compared. For $\Delta_E > 1$, the step density in the [110] direction is greater than in the [$\bar{1}$10], which corresponds to an elongation of islands on the terraces. For $\Delta_k > 1$, however, and even up to $\Delta_k = 10$, there is no change in relative step densities. We can therefore con-

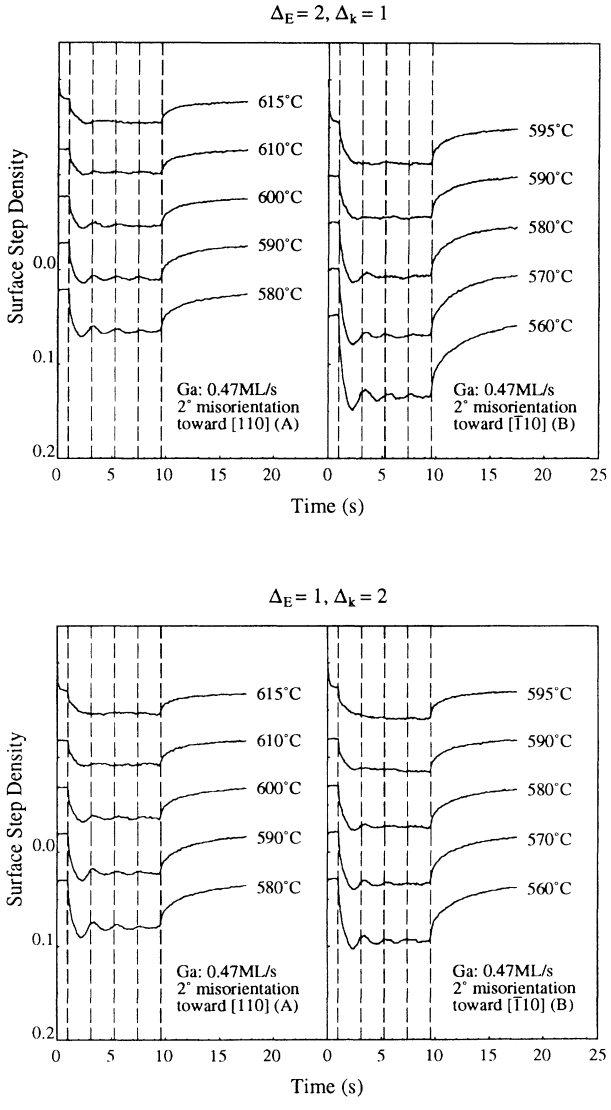

FIG. 8. Simulated surface step density evolution on A and B surfaces with $\Delta_E = 2$ and $\Delta_k = 1$ (top) and $\Delta_E = 1$ and $\Delta_k = 2$ (bottom). The growth rate is 0.47 mL/s.

clude that while both Δ_k and Δ_E can change T_c, only Δ_E can influence island shape. We have illustrated this (Fig. 10) by a simulation of surface morphology on A and B surfaces after recovery, using identical growth conditions for $\Delta_E=2$ and $\Delta_k=2$. With the former, step edges are very different on A and B surfaces, while there is very little difference with the latter. If we compare these results with STM observations,[5] it is quite clear that there is very close qualitative similarity with the simulated morphologies for $\Delta_E=2$, in that step edges are much rougher on the B surface than the A.

The way in which the growth-mode transition is induced by each effect ($\Delta_E>1$ or $\Delta_k>1$) is explained schematically in Fig. 11. For $\Delta_E>1$, islands formed on the terrace are elongated along [$\bar{1}$10], which means that on A surfaces (steps parallel to [$\bar{1}$10]), the islands do not coalesce with the steps until near monolayer completion and cluster formation can continue until the mobility of single adatoms becomes very high. On B surfaces, however, islands can coalesce with steps well before monolayer completion, which effectively reduces the terrace width since steps elongate normal to their edges, thereby suppressing island formation. Oscillations therefore damp rapidly on B surface and T_c is always higher on A than B surfaces.

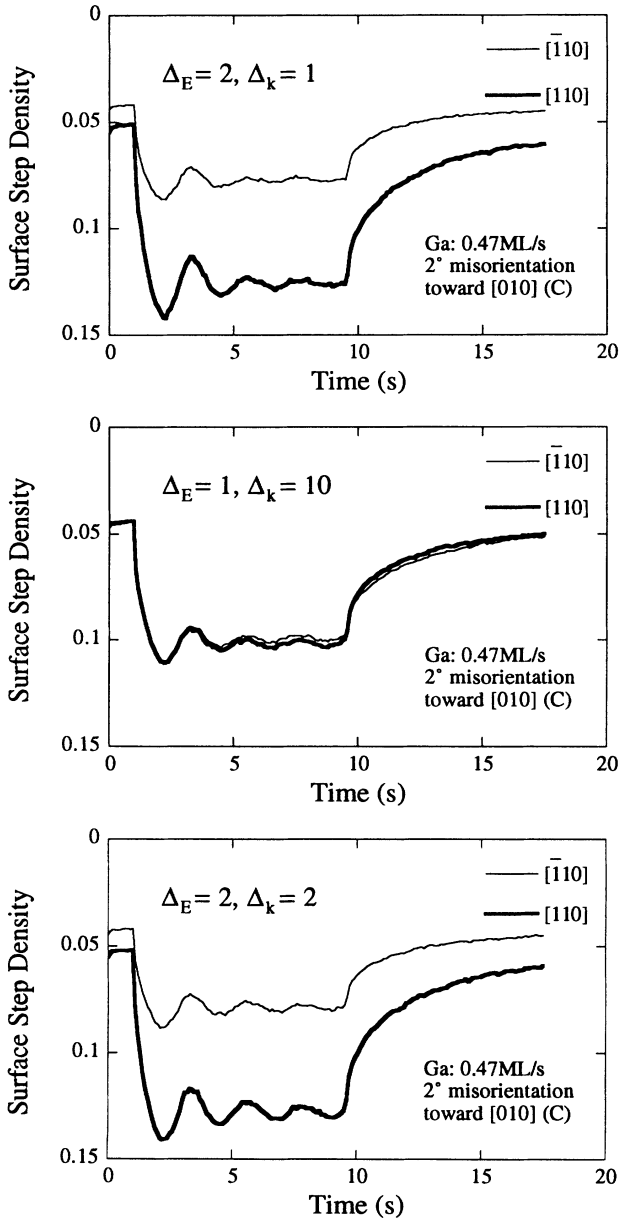

FIG. 9. The simulated surface step density evolutions of Ga-terminated steps (in the [110] direction) and As-terminated steps (in the [$\bar{1}$10] direction) with $\Delta_E=2$ and $\Delta_k=1$ (top), $\Delta_E=1$ and $\Delta_k=10$ (middle), and $\Delta_E=2$ and $\Delta_k=2$ (bottom).

If $\Delta_k>1$, the final conclusions are the same, but we have to postulate a different mechanism for the growth-mode transition. In this case, adatoms can more easily reach step edges on B surfaces, so that again T_c is lower there. Morphological anisotropy could be introduced in this way only if the steps acted as perfect sinks for adatoms, but we have shown in a separate publication[14] that this is not so, which implies that migration anisotropy alone cannot account for all of the observations.

Finally, we introduced both possible causes of anisotropy simultaneously into the simulations to investigate their interaction. For $\Delta_E=2$ and $\Delta_k=2$, the difference in T_c is enhanced, but there is no change in the island morphology with respect to $\Delta_E=2$ and $\Delta_k=1$, providing further evidence that the morphology is determined primarily by Δ_E. An interesting effect is observed for $\Delta_E=2$, $\Delta_k=0.5$, where on the C surface the result is identical to $\Delta_E=2$ and $\Delta_k=2$ because the two different step directions exist together, but on A and B surfaces the effect is different, as illustrated in Fig. 12. This figure shows the simulated growth mode on all three surfaces for $\Delta_E=2$ and $\Delta_k=0.5$. Since $\Delta_E>1$ increases T_c, while $\Delta_k<1$ reduces it, differences in T_c between the three surfaces are reduced, but the first oscillation on the B surface is enhanced. The effect is to produce a result very similar to that obtained experimentally (Fig. 2), provided the diffraction effects associated with the A surface, which we have already discussed, are ignored.

The anisotropy of the delay to the first maximum in the RHEED intensity oscillations provides additional experimental evidence to support the concept of nearest-neighbor bonding energy anisotropy. We have reported separately[14] a systematic study of this phenomenon, which showed that the delay is a measure of that fraction of the incident flux which is directly incorporated into the staircase steps below T_c. Figure 13 shows an Arrhenius plot of this incorporation rate, which illustrates that direct adatom incorporation is faster into B steps than A steps at the same temperature, but the activation energy for A step incorporation is very much higher than for B steps. The clear implication is that the origin of the anisotropic growth-mode transition is strongly associated with nearest-neighbor barrier-energy considerations.

VI. CONCLUSIONS

The misorientation-direction dependence of the transition from growth by the formation and coalescence of

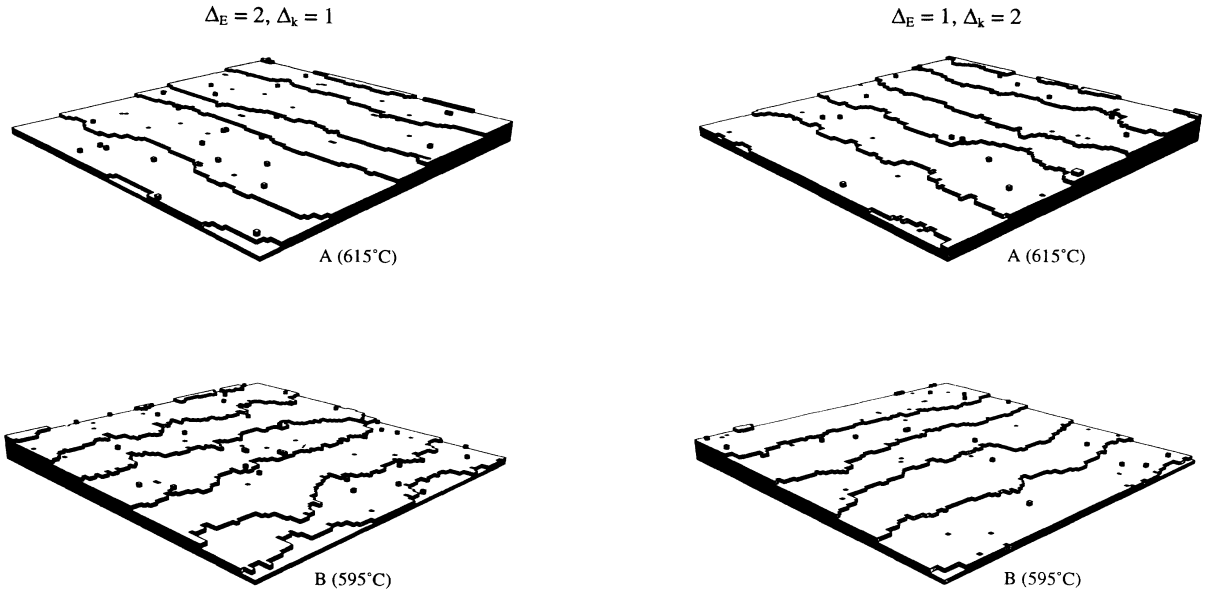

FIG. 10. Simulated surface morphology on A and B surfaces at the highest temperature in Fig. 8 with $\Delta_E = 2$ and $\Delta_k = 1$ (top panels) and $\Delta_E = 1$ and $\Delta_k = 2$ (bottom panels).

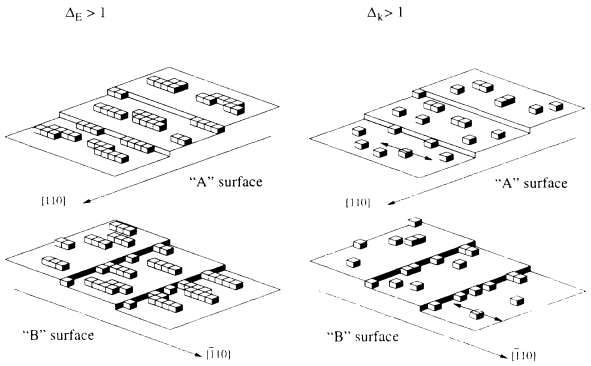

FIG. 11. Schematic illustration of the different mechanisms of the growth-mode transition. $\Delta_E > 1$ and $\Delta_k = 1$ (left) and $\Delta_E = 1$ and $\Delta_k > 1$ (right).

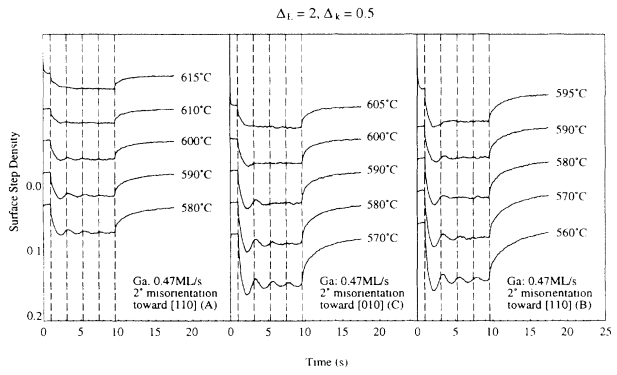

FIG. 12. Simulated surface step density evolutions on A, B, and C surfaces with $\Delta_E = 2$ and $\Delta_k = 0.5$.

two-dimensional clusters to growth by step advancement on vicinal GaAs(001) has been studied by comparing RHEED measurements with Monte Carlo growth simulations. There are two possible origins of this anisotropy: the anisotropic mobility of single adatoms and the anisotropic incorporation of adatoms into the steps. To investigate what effect each would have on the growth-mode transition and morphology, we introduced the anisotropies into our growth model both separately and simultaneously.

Because of diffraction effects, we were unable to make the types of direct comparisons between the step density

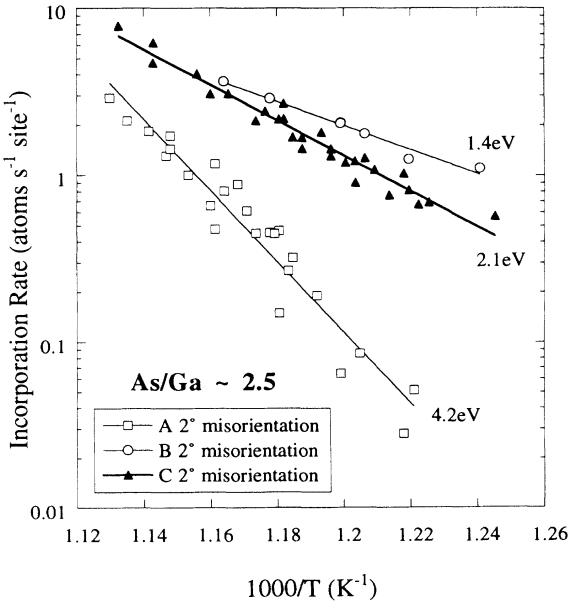

FIG. 13. Arrhenius plot of the incorporation rate at steps on A, B, and C surfaces.

and the RHEED intensity during growth as we did in our earlier work.[10] Had we been able to do so, the features of the RHEED data as the substrate temperature approaches T_c would have allowed a more detailed examination of the origins of the anisotropy, particularly whether there is a barrier component to adatom anisotropy, which has a different temperature dependence than the frequency anisotropy. Nevertheless, by appealing to surface morphologies produced by the two models and to measurements of the step propagation rate,[14] we were able to identify characteristic differences between the two anisotropies.

Although the transition temperature can be changed by both processes, the *magnitude* of the misorientation-direction dependence of T_c does place bounds on the extent of the anisotropy due to each process. Thus, anisotropic morphological features such as step roughness and elongated islands are only reproduced by anisotropic incorporation kinetics. The step propagation rate, as measured by the first maximum delay in RHEED oscillations, on the other hand, strongly supports anisotropic incorporation into steps, because it identifies the attachment and detachment processes at the step edges as being rate determining for the incorporation of adatoms into the growth front.[14] This conclusion was also reached by Zandvliet *et al.*[22] based on RHEED measurements and Monte Carlo simulations for vicinal Si(001). We can therefore safely conclude from our investigation that morphological anisotropy derives principally from the anisotropy of nearest-neighbor bonds rather than the migrational anisotropy of single adatoms. This does not of course rule out the possibility of anisotropic migration, but if it exists the higher mobility direction is likely to be orthogonal to that reported by Ohta, Kojima, and Nakagawa[6] on the basis of T_c measurements alone. If there is a rapid direction it is parallel to the As-As dimer rows (along the [110] direction in Fig. 6) and Ga adatoms will be chemisorbed on surface As atoms. This is such as to reduce the anisotropy by bonding effects.

ACKNOWLEDGMENTS

One of us (T.S.) would like to acknowledge the support of the Committee of Vice-Chancellors and Principals of the Universities of the United Kingdom and the Matsushita Research Institute. The support of Imperial College and the Research Development Corporation of Japan under the auspices of the "Atomic Arrangement: Design and Control for New Materials" Joint Research Programme is also gratefully acknowledged.

*Present address: Department of Electrical and Electronic Engineering, University College, London WC1E 7JE, United Kingdom.

[1]J. H. Neave, P. J. Dobson, B. A. Joyce, and J. Zhang, Appl. Phys. Lett. **47**, 100 (1985).

[2]P. M. Petroff, A. C. Gossard, and W. Wiegmann, Appl. Phys. Lett. **45**, 620 (1984).

[3]C. Weisbuch, R. Dingle, A. C. Gossard, and W. Wiegmann, Solid State Commun. **38**, 709 (1981).

[4]P. M. Petroff, J. M. Gaines, M. Tsuchiya, R. Simes, L. A. Coldren, H. Kroemer, J. H. English, and A. C. Gossard, J. Cryst. Growth **95**, 260 (1989).

[5]M. B. Pashley, K. W. Haberern, and J. M. Gaines, Appl. Phys. Lett. **58**, 406 (1991).

[6]K. Ohta, T. Kojima, and T. Nakagawa, J. Cryst. Growth **95**, 71 (1989).

[7]P. R. Pukite, S. Batra, and P. I. Cohen, SPIE **95**, 269 (1989).

[8]T. Shitara and T. Nishinaga, Jpn. J. Appl. Phys. **28**, 1212 (1989).

[9]M. Kawabe and T. Sugaya, Jpn. J. Appl. Phys. **28**, L1077 (1989).

[10]T. Shitara, D. D. Vvedensky, M. R. Wilby, J. Zhang, J. H. Neave, and B. A. Joyce, Appl. Phys. Lett. **60**, 1504 (1992); T. Shitara, D. D. Vvedensky, M. R. Wilby, J. Zhang, J. H. Neave, and B. A. Joyce, preceding paper, Phys. Rev. B **46**, 6815 (1992).

[11]J. Zhang, J. H. Neave, P. J. Dobson, and B. A. Joyce, Appl. Phys. A **42**, 317 (1987).

[12]J. H. Neave, B. A. Joyce, and P. J. Dobson, Appl. Phys. A **34**, 179 (1984).

[13]H. Toyoshima, T. Shitara, J. Zhang, J. H. Neave, and B. A. Joyce, Surf. Sci. **264**, 10 (1992).

[14]T. Shitara, J. Zhang, J. H. Neave, and B. A. Joyce, J. Appl. Phys. **71**, 4299 (1992).

[15]T. Shitara, J. Zhang, J. H. Neave, and B. A. Joyce, in *Epitaxial Crystal Growth,* edited by E. Lendvay (Trans Tech, Switzerland, 1991), pp. 332–337.

[16]S. Clarke and D. D. Vvedensky, Phys. Rev. Lett. **58**, 2235 (1987).

[17]J. D. Weeks and G. H. Gilmer, Adv. Chem. Phys. **40**, 157 (1979).

[18]P. Chen, J. Y. Kim, A. Madhukar, and N. M. Cho, J. Vac. Sci. Technol. B **4**, 890 (1986).

[19]K. Shiraishi (unpublished).

[20]A. Rockett, Surf. Sci. **227**, 208 (1990).

[21]Y.-W. Mo and M. G. Lagally, Surf. Sci. **248**, 313 (1991).

[22]H. J. W. Zandvliet, H. B. Elswijk, D. Dijkkamp, E. J. van Loenen, and J. Dieleman, J. Appl. Phys. **70**, 2614 (1991).

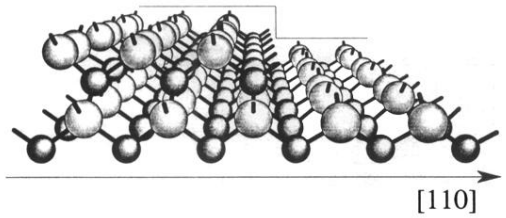

A surface (Ga terminated)

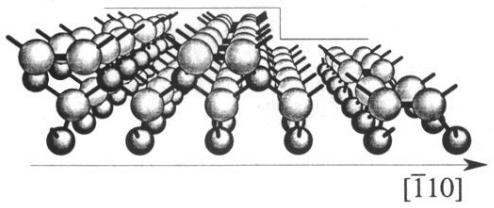

B surface (As terminated)

FIG. 6. Schematic illustration of the GaAs(001) 2×4 reconstruction and the different step structures.